Observation and Analysis of a High Frequency MHD Activity during Sawteeth in KSTAR Tokamak

C.M.Ryu[1], M.H.Woo[1], M. J. Hole[2], J.K. Bak[3], and NFRI operation team[3]

[1] POSTECH, Pohang, Korea; [2] Research School of Physical Sciences and Engineering, Australian National University, Canberra, Australia; [3] NFRI, Daejeon, Korea

E-mail contact: ryu201@postech.ac.kr

Abstract. During the second campaign of the KSTAR operation in 2009, off-axis ECRH/ECCD heating was applied to the high-field side of the q=1 surface during a set of four plasma discharges. In these experiments we have observed high frequency MHD activity which varies from 4 to 6 kHz in both temperature and magnetic fluctuation. Our analysis suggests this is the electron fishbone instability.

1. Introduction

We report on a set of four successful discharges; #2173, #2176, #2178, #2179, #2181, acquired during the second 2009 campaign of KSTAR operations attempted to find a signature of the electron fishbone instability. Maximum current of 250kA was reached for a 3.6s pulse length. For all discharges, the TF coil current was set to 20.3kA, giving a vacuum toroidal magnetic field at R=1.80 at the plasma geometric axis of B_t= 2.03T.A 250kW electron cyclotron harmonic (ECH) system with 110.06 GHz gyrotron was used for the second harmonic heating. The shooting position of ECH is located at R=1.86 m and the resonance position is set at approximately 1.8m for the poloidal injection ($k_\parallel \approx 0$). Electron cyclotron current drive (ECCD) was also available for #2181. For this discharge, the injection angle was set to -10° in the toroidal direction (counterclockwise in the co-current direction), and also 17cm below the horizontal axis of plasma poloidally. Both ECH and ICRF powers are injected at -160ms as pre-ionization and used secondary gas puffing to control the initial plasma density and the current growth rate to assist the start up of the plasma.

In the experiment we tried to find a signature of the electron fishbone instability by using ECH off-axis heating and ECRH/ECCD current drive at high field side of q=1 surface. We have identified, first, 1) the sawtooth oscillation of the temperature, and next, 2) the radius of q=1 surface from the rough information about the inversion of ECE channel signal data, and, finally, 3) high frequency MHD activity.

In this paper we report on high frequency MHD mode found in the KSTAR experiment during the ECCD/ECRH. The high frequency MHD is identified as the electron-fishbone instability for the following reasons: 1) The signal appears to be independent of sawtooth event, 2) Off-axis high field side heating provides supra-thermal electrons which can resonantly interact with MHD modes. 3) Close correlation of such high frequency activity with ECRH/ECCD heating is shown. 4) The observed frequencies correspond to the

computed electron resonant precession frequency.

The precession direction of barely trapped electrons in plasmas with small or reversed shear can be reversed (drift-reversal), and move in the ion-diamagnetic direction. Such electrons can provide a source of drive for the kink mode [1]. The electron fishbone instability was first observed in DIII-D tokamak by K.L.Wong *et al* [2]. They used NBI to make reversed shear and high-field side ECCD heating to generate barely trapped hot electrons. Electron fishbone activity has also been observed in pure ECRH-only heated plasmas [3, 4], LH current drive in FTU [5, 6] and Tore Supra [7] with drift-reversal of barely circulating electrons. Excitation of electron fishbone with barely circulating particle on the low field side ECRH heating is verified in HL-1M tokamak [4]. Recently, in HL-1M tokamak plasmas, Wang *et al.* [8] found that the precession direction is always negative in reverse shear plasmas.

During off-axis ECH heating and ECCD current drive on a high field side of q=1 surface, we have found a high frequency MHD mode. Fishbone-like MHD bursts and activities are found in the ECE signal data and the Mirnov coil data. We present the typical signals together with the SVD data analysis which we used to identify the mode frequency and mode numbers. To see whether our electron fishbone-like MHD mode is driven by resonant electrons, we have carried out a kinetic analysis of the fishbone instability and estimated it's resonance frequency. The remainder of this paper is structured as follows: Sec. 2 describes the KSTAR experiment, Sec. 3 presents a theoretical calculation of the precession frequency, and Sec. 4 contains concluding remarks.

2. KSTAR Experimental Setup

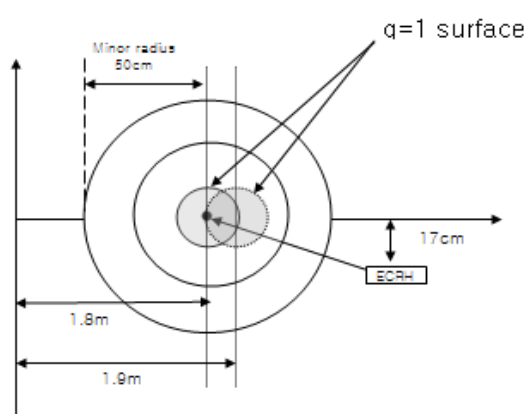To make ECH heating off-axis on the high field side, we fixed the ECRH/ECCD position, but moved the plasma to an appropriate position so that ECRH/ECCD heating position passes high field side of q=1 surface. At plasma startup, the radial position of the geometric axis of the circular cross-section plasmas, R_p, was set to 1.8m. A digital plasma control system (PCS) was used to vary the currents in the poloidal field coils, thereby changing the vertical magnetic field, and move the plasma inward or outward. A schematic of the plasma cross-section, identifying the q=1 surface relative to the geometric axis is shown in Fig. 1. During the plasma discharge we tried to move plasma position from 1.8m to 1.9m linearly with time over the interval 0~3.0s, where ECH stop at 2.8s. The plasma cross-section was circular, with minor radius 0.5m, and a monotonic safety factor profile-delete, with minimum q, q_{min} ~1.

Fig. 1.   Systemic settings of experiment.

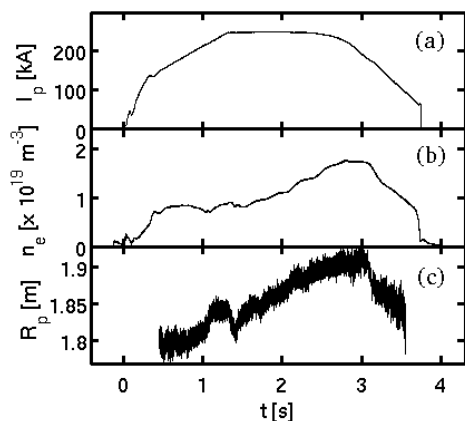*Fig. 2. Evolution of (a) plasma current Ip, (b) line averaged electron density ne and (c) plasma geometric-axis position R_p for discharge #2181.*

TABLE 1: Plasma parameters for discharge # 2181

I_tf(kA)	20.4
Ip(kA)	250.1
Pulse > 0.1kA(msec)	3761.1
Ne(10^19/m^2)	1.8
Te(KeV)	2.0
Pressure(mbar)	1.7E-5
ECH_P(kW)	256.6

Figure 2 shows the evolution of plasma current I_p, line averaged electron density n_e and plasma geometric axis R_p for discharge #2181. The electron density was measured with interferometer which gives line averaged density of the plasma, and the plasma position is measured by using a simple two B-probe estimator similar to that deployed in EAST [9] that utilizes knowledge of the PF coils and midplane coils to estimate the plasma radial response. In discharge #2181 the plasma current plateau occurs at 250 kA. The increase in density up to a maximum of $1.8 \times 10^{19} \, m^{-2}$ at 3.0s occurs principally because the plasma geometric axis moves outboard towards the ECRH shooting position at R=1.86m. Table 1 lists some plasma parameters for this discharge.
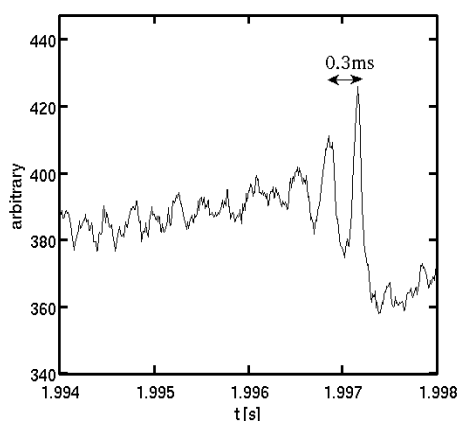

Fig. 3. ECE data for channel 2 at radial chord R=1.81m in discharge #2181.

An electron cyclotron emission (ECE) diagnostic affords line integrated measurements of the electron temperature. These reveal a sawtooth oscillation when the plasma reaches sufficiently high current (~200kA) and temperature (~1keV). Figure 3 shows the collapse of a sawtooth event near 2.0s of channel 2 of the ECE diagnostic, located at a radial chord R=1.81m. We have identified the sawtooth oscillation period to be 0.3 ms. This can be compared to the collapse time from the classical

Kadomstev model, with formula $\tau_k = \sqrt{\tau_\eta \tau_A}$, where τ_η resistive diffusion time is and τ_A is

Alfvenic time. In our ECCD experiment, flat-top current has reached 250 kA and maximum

temperature is 2.5 keV with density 1.5×10^{19} m^{-3}, and the toroidal magnetic field at the geometric axis is B_t=2T. Using such parameters we estimate the sawtooth period as $\tau_k \approx 0.15$ ms. This compares reasonably to the measured oscillation period of 0.3ms.

Figures 4(a) and 4(b) show two different phases of sawteeth from ECE02 channel at the same radial position (1.81m) at two 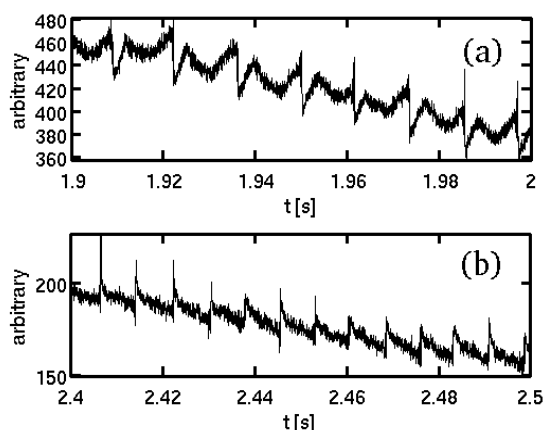different times: 2.0s and 2.5s. From the measurement of plasma position as shown in Fig. 2(c), the plasma center is at 1.86m at 2.0s and moves to 1.9m at 2.5s. In Fig. 2(b) we can see a clear phase reversal near 2.4s compared to 2.0s: this phase reversal is consistent with the q=1 surface moving outboard of the R=1.81m. Given the plasma geometric axis is located at 1.9m at 2.5 s, we hence conject the q=1 surface has a minor radius of less than 10cm. During the time interval 2.0s to 2.5s, the total plasma current has been kept in a flat top and ECH heating has sustained.. This allows high-field side off-axis ECRH heating inside the q=1 surface.
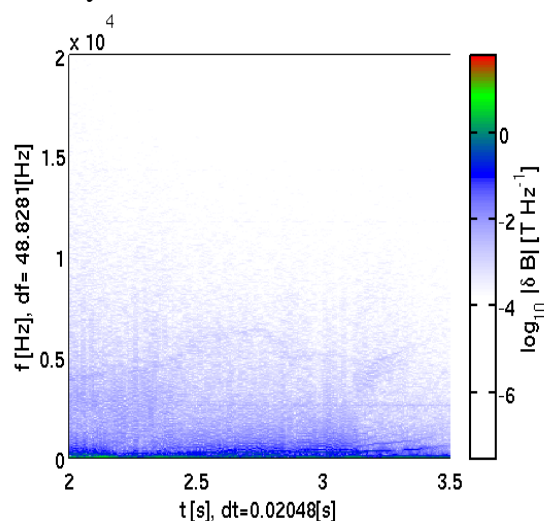

Fig. 4. ECE channel 2 signal at R=1.81m at (a) 2.0s and (b) 2.4s.

Two main different types of coherent wave activity were observed: the sawtooth, comprising the low frequency, f~100Hz bands and harmonics which is a clear indication of the sawtooth; and a weaker, coherent wave at 4-6kHz between 2.4 and 2.7s. Figure 5 shows a spectrogram of the ECE data of channel 2 at R=1.81. Similar activity is also observed in other channels of the ECE data located at other high field positions. A spectrogram of Mirnov coil data also shows the coherent signal at 4-6kHZ, suggesting that this mode is global in radial extent. At 2.8s when the ECRH power falls to zero and the wave oscillation falls from 6 kHz to 5 kHz in correlation with ECRH power.

Fig. 5. Spectrogram of ECE data at R=1.81 m. The low frequency (~100Hz) sawtooth and harmonics are evident, as well as a higher frequency 4-6 kHz coherent mode.
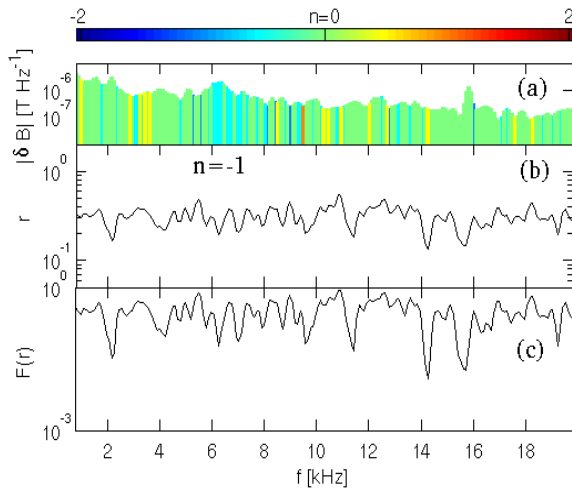
Fig. 6. Toroidal mode number n=1 from toroidal spaced Mirnov coils. Panel (a) shows the perturbed field strength and mode number n, panel (b) the residue, and panel (c) the probability that the mode was generated y Gaussian noise.

The toroidal mode number of the 4-6 kHz wave has been identified from a Fourier-SVD analysis [11] for a set of two Mirnov coils spaced 90° apart in toroidal angle. For this toroidal angle spacing the alias number is 2. Figure 6 shows the extracted toroidal mode number at 2.7s, identifying the feature at 6kHz to have a dominant toroidal mode number |n|=1.   The residue to the fit drops either side of the signal, and the fit is consistent across the peak, providing evidence that the mode number is correct to within the alias.   We have also mapped the residue to the probabality that Gaussian noise could generate a fit with this residue or less, and there is only a 10% probability that the feature at 6kHz could be generated by noise.   Although a set of four poloidally spaced Mirnov coils exists, the equilibrium reconstruction is not available, and so we have been unable to compute the poloidal angle in straight field line coordinates, and hence unable to compute poloidal mode numbers.

3. Theoretical Interpretation

Dispersion relation for internal kink mode with presence of resonant particle is given as

$$\delta W_c + \delta W_k - i\frac{\omega}{\omega_A} = 0 \qquad (1)$$

Where $\omega_A = V_A / \sqrt{3} s R_0$ is shear Alfven frequency. Here V_A is Alfven velocity and s is the magnetic shear at q=1 surface. Here δW_c is plasma energy due to ideal kink mode and δW_k wave-particle resonant kinetic contribution and third term is inertial contribution. From the ideal kink mode growth rate expression it is possible to get contribution from core with

$$\gamma_I = -\frac{\sqrt{3}\pi\omega_A}{q''R^2}[1-q(0)](\beta_p^2 - \frac{13}{144}) \qquad (2)$$

For the wave particle resonance part, from Gyrokinetic theory it is given as [11]

$$\delta W_k = 2^{7/2} \frac{m\pi^2}{B_0^2 r_s^2} \int_0^{r_s} r dr \int d(\alpha B) \int \frac{dE E^{5/2} K_2^2 \omega}{K_b(\omega_d - \omega)} (\frac{\partial}{\partial E} - \frac{1}{mr\omega_c \omega_d} \frac{\partial}{\partial r}) F \qquad (3)$$

Where F is background distribution function and ω_d is the precession frequency of resonating particle. Solving for dispersion relation (1) gives $\omega \approx \frac{\omega_d}{2}$ which states that internal kink mode in tokamak will have the same order of electron precession frequency for both barely trapped and circulating electrons.

To apply the above theory to KSTAR, we estimate the precession frequency for both barely trapped and circulating electrons, assuming that the electron has a parallel energy of 40keV. Due to high electron energy, relativistic effect may become important. Now we have used KSTAR parameters with $R_0 = 180cm$, $r_s = 10cm$, inverse aspect ratio $\varepsilon = 0.056$, Bt=2.0T and assumed small negative magnetic shear with s=-0.02. Defining $u_\phi = \gamma W_\parallel$ as thermal momentum of relativistic electrons normalized momentum $U = u_\phi / c$ and parallel energy have such relation.

$$\frac{E_\parallel}{m_0 c^2} (1 + \frac{\sqrt{1 + k^2 U^2 / 2\varepsilon} - 1}{\sqrt{1 + U^2} - 1}) = \sqrt{1 + U^2 (\frac{k^2}{2\varepsilon} + 1)} - 1 \qquad (4).$$

Here, $k = \frac{2\varepsilon u_\perp^2}{u_\phi^2}$ is related to bouncing angle for trapped electrons. In Fig. 12 solid line is real velocity of electrons versus k where relativistic effects are included and it is clear that they do not exceed speed of light. Bouncing frequency of barely trapped and circulating electrons are given as[8]
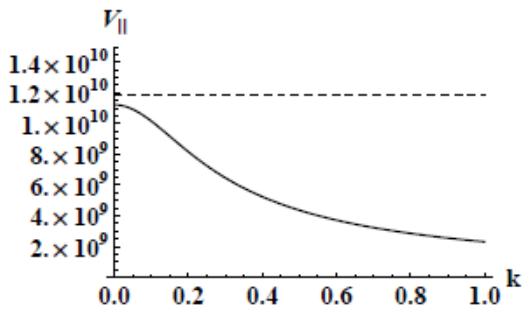

Fig. 7. Parallel velocity versus k.

$$\omega_{dt} = \frac{2\Omega_0 p_\alpha}{\gamma \Omega_p m_0 R^2} \{\frac{E(k_1)}{K(k_1)} - \frac{1}{2} + 2s[\frac{E(k_1)}{K(k_1)} - (1 - k_1^2)]\}$$

$$\omega_{dc} = \frac{u_\phi^2 G_c}{2\gamma \Omega_p r_s R_0} [\frac{E(k)}{K(k)} - (1 - \frac{k^2}{2}) + 2s\frac{E(k)}{K(k)}]$$

Here $k_1 = k^{-1}$, Ω_0 is cyclotron frequency at the magnetic axis, Ω_p is poloidal cyclotron frequency and $p_\alpha = \frac{1}{2} m_0 \Omega_0 \rho^2$ where ρ gyro-radius of hot thermal electron. $E(k)$ is complete elliptical integral of second kind and $K(k)$ is the first kind elliptical integral. In Fig. 15(a) and 15(b) we have numerically plotted these two frequencies.

From Fig. 8(a) we can see that the precession frequency is a rather sensitive function of a

pitch angles that drift-reversal occurs below $k_1 < 0.9$. However, from Fig. 8(b) it is clear that barely circulating particle is always precessing in ion diamagnetic direction and for large range of pitch angle their frequency is below 10 kHz, varying from 4 to 7 kHz. This is consistent with the observed MDH activity signal. We conclude from this analytical result that in the excitation of the electron fishbone, barely circulating electrons may contribute more than barely trapped particle [8]. But due to KSTAR experimental set up, high field side off-axis heating can generate hot electrons with both barely trapped and circulating electrons and there is no direct way of measuring to distinguish the each portion of trapped and circulating particles.
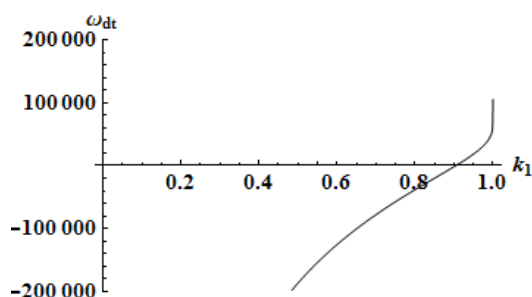
Fig. 8a. Trapped particle precession frequency.
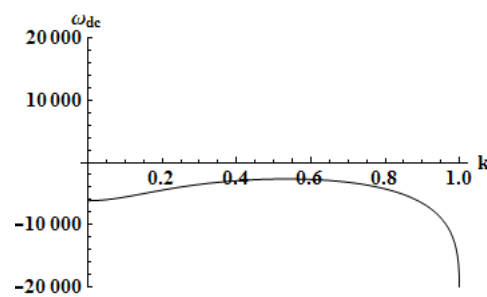
Fig. 8b. Circulating particle precession frequency.

4. Summary

In summary, by examining temperature perturbation by ECE signals and magnetic field fluctuations by Mirnov Coil, we have found that there is a fishbone-like high frequency MHD mode driven by ECRH/ECCD, which varies from 4000Hz to 7000Hz appearing in a time period between 2.4 to 2.8 seconds when the ECRH/ECCD heating applied on a high field side.

By examining the inversion of sawtooth oscillation we have identified that q=1 surface is approximately located at 10 cm. The mode number has been identified using the Fourier SVD technique as $|n|$=1 with a frequency 5800Hz, near 2.6s. We conjecture that the appearance of the signal with frequency 4 to 7 kHz is mainly due to m=1 kink instability driven by high energy electrons from ECH where instability threshold is mainly dependent on the radial profile of hot electron pressure. Theoretical estimation of the trapping and passing frequency of electrons is found to be in the same range of the observed signals. Thus we draw a conclusion that such mode is excited by resonance of an (n,m) = (1,1) internal kink mode with drift-reversed trapped or circulating particles.

Acknowledgement

References

[1] ZONCA F.,et al., Nucl. Fusion **47**(2009), 1588–1597.

[2] WONG K.L., et al.,Physical Review Letters **85**(2000), 5.

[3] DING X.T., et al., Nucl. Fusion **42**(2002) 491.

[4] CHEN W., et al., Nucl. Fusion **46**(2009), 6.

[5] SMEULDERS P., et al., 2002 Fast MHD Analysis on FTU Proc. 29th EPS Conf. on Plasma Physics Controlled Fusion (Montreux, Switzerland, 2002) vol 26B (ECA) D-5.016 and http://epsppd.epfl.ch/Montreux/start.htm 1596 Electron fishbones: theory and experimental evidence

[6] ROMANELLI F., et al., 2003 Overview of the FTU results Proc. 19th Int. Conf. on Fusion Energy 2002 (Lyon, France, 2002) (C&S Papers Series No 19/C) (Vienna: IAEA) CD-ROM file Ov/4-5 and
www.iaea.org/programmes/ripc/physics/fec2002/html/fec2002.htm

[7] MAGET P., et al., Nucl. Fusion **46**(2006), 797.

[8] WANG Z.T., Nucl. Fusion **47**(2007), 1307–1310.

[9] LEUER. JA, et al., "EAST First Plasma: Design, Simulation & Experimental Results", Presented at the 49th American Physical Society Meeting Division of Plasma Physics, Orlando, Florida, Nov 12-16, 2007.

[10]WHITE R.B., et al., Phys. Fluids **28**(1985), 278.

[11]HOLE M.J., and L. C. Appel, PPCF **49**(2007), 1971-1988.